Journal Pre-proofs

A dual-objective trade-off approach to decide the optimum design parameters for internal cooling load calculation

Yan Ding, Junchu Li, Kuixing Liu, Shen Wei, Wanyue Chen, Shuxue Han

Please cite this article as: Y. Ding, J. Li, K. Liu, S. Wei, W. Chen, S. Han, A dual-objective trade-off approach to decide the optimum design parameters for internal cooling load calculation, *Energy & Buildings* (2022), doi: https://doi.org/10.1016/j.enbuild.2022.112230

This is a PDF file of an article that has undergone enhancements after acceptance, such as the addition of a cover page and metadata, and formatting for readability, but it is not yet the definitive version of record. This version will undergo additional copyediting, typesetting and review before it is published in its final form, but we are providing this version to give early visibility of the article. Please note that, during the production process, errors may be discovered which could affect the content, and all legal disclaimers that apply to the journal pertain.
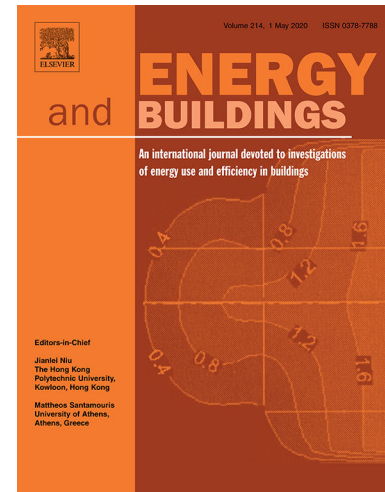
A dual-objective trade-off approach to decide the optimum design parameters for internal cooling load calculation

Yan Ding[1,2], Junchu Li[1], Kuixing Liu[3,*], Shen Wei[4], Wanyue Chen[1], Shuxue Han[1]

[1]School of Environmental Science and Engineering, Tianjin University, Tianjin 300072, China
[2]Key Laboratory of Efficient Utilisation of Low and Medium Grade Energy, MOE, Tianjin University, Tianjin 300072, China
[3]School of Architecture, Tianjin University, Tianjin 300072, China
[4]The Bartlett School of Sustainable Construction, University College London (UCL), 1-19 Torrington Place, London WC1E 7HB, United Kingdom

Corresponding Author. E-mail address: liukuixing1@sina.com (K. Liu)

Abstract

The building design cooling load is the basis of sizing the air-conditioning equipment, but the extreme values are always used as the referenced design parameters for occupants, lighting and equipment respectively without considering the relationship between the internal load sources which will result in an oversized equipment. Based on the measured data in existing buildings, the Copula function is used to explore the joint occurrence probability of the internal disturbances. In view of the deviation of the calculated cooling load from the extreme cooling load, the unguaranteed rate is established. Aiming to balance the maximum joint probability and the minimum unguaranteed rate, a dual-objective trade-off approach with the genetic algorithm and TOPSIS method is proposed to seek the optimum solution from the Pareto Fronts to provide references for internal load design parameters. The results show that there is a big deviation between the design values and trade-off results, especially the recommended values of lighting power density in the design standards are at least 26% higher than the trade-off results. And the energy consumption for internal disturbances can be at least reduced by 12.1% using the trade-off approach.

Keywords

internal loads, trade-off approach, unguaranteed rate, internal disturbances, joint probability distribution

1. Introduction

1.1 Research background

It is well known that buildings account for nearly 40% of overall global energy consumption [1], and this number is even higher in China (i.e. 46%) [2]. This huge energy consumption is mostly coming from the running of HVAC systems to provide comfortable indoor environment [3], and their contribution can be up to 40% of overall building energy consumption [4]. In China, cooling buildings by HVAC systems has a significant contribution [5,6]. In many buildings, however, mechanical cooling systems do not always operate under the optimal performance conditions [7]. This is mainly due to ensuring that the energy system has sufficient capacity, the system is usually oversized with a larger safety factor than that actually needed [8], which results in the equipment operating with a low operational efficiency most of the time, causing damage to the equipment and unnecessary energy lost [9]. As for the cooling water systems, a design safety factor of up to 20% is usually applied which results in an increased operating cost [10]. To ensure their performance, these systems need to be properly designed, selected and sized, based on an accurately estimated design cooling load [11].

In conventional cooling load calculations, extreme statistical values with corresponding safety margins are widely adopted when selecting design parameters, in order to meet the load demand under extreme conditions [12]. If the selected design values are too high, the plant will be oversized, resulting in an increased initial investment and

decreased plant operational efficiency [13]. If the selected design values are too low, the system capacity may not meet actual demand during operational time, especially at extreme conditions [14]. Additionally, a properly selected safety margin is also important for ensuring acceptable indoor thermal environment with minimized energy consumption. To achieve these targets, the values of relevant design parameters need to be selected as close as to actual conditions [11].

1.2 Uncertainty analysis in cooling load calculation

Many existing studies have suggested that the values of design parameters for calculating the cooling load of buildings are different from the actual values at operation stage [11, 15, 16, 17], due to many uncertainties [18], such as meteorological parameters, envelope parameters and occupant-related parameters [19]. In recent years, due to the increasing improvement of building thermal insulation, the influence from outdoor weather parameters has been well controlled [20]. The internal loads, however, continuously increase in modern buildings due to the higher dependence of human activities on electrical equipment [21], and this part is closely linked to room occupancy and occupant behavior [22]. Due to the stochastic characteristics of these two parameters, the internal loads, including occupancy, lighting power density and equipment power density, are difficult to decide, and this may lead to a significant deviation between design and actual values [18].

To quantify the stochastic nature of room occupancy and occupant-centric internal disturbances in load calculation, many researchers have carried out research in predicting room occupancy, lighting load and equipment load. Tagliabue et al. [23] have proposed a probabilistic modeling approach describing occupancy related parameters using probability distributions. Ding et al. [24] have proposed a correction coefficient based on questionnaires to modify the occupancy rate and this approach achieved a reduction of cooling load by 35.9%, with a high assurance rate. Zhou et al.

[28] developed a stochastic lighting model based on lighting energy use data from 15 large office buildings which can generate more accurate lighting schedules to improve simulation accuracy. Sarfraz et al. [30] used the experimental methodology to measure heat gain values for different office equipment to update heat gain tables. Zhang et al. [32] have proposed a probabilistic approach for describing the spatial distribution characteristics of internal heat gains from occupants, lighting, and plug loads respectively, and their results showed that the calculated building cooling load was close to the actual peak cooling load. Table 1 has summarized existing literature in terms of quantifying the uncertainties of internal disturbances.

Table 1: Existing literature in terms of quantifying the uncertainties of internal disturbances

Internal disturbances	Quantified results	Literature
Occupancy	Occupancy rate Occupancy schedule	[21-27]
Lighting load	Lighting schedules Lighting energy consumption	[28, 29]
Equipment load	Real-time equipment usage profiles Equipment energy consumption	[16, 30, 31]
Internal heat gain from occupants, lighting and equipment (separately)	Calibrated value of internal disturbances Internal cooling load	[10, 15, 21] [32-36]

1.3 Research gap and scientific contributions

Existing studies on the uncertainties of building internal load mainly focused on quantifying the individual influence from occupancy, lighting and equipment, as shown in Table 1, but have not yet considered the joint occurrence probability between them. For example, it has been well justified that both equipment usage and lighting usage are

highly dependent on the occupancy rate of the building [37]. Without considering these dependencies, the safety margins of these interlinked parameters will be treated separately so the difference between the design condition and the actual condition will be enlarged. In the design calculation process of building cooling load, the maximum values of these parameters are usually used to cover extreme conditions. However, the probability of a single parameter reaching its extreme value is small, nevertheless when all three parameters reaching their extreme values simultaneously. Therefore, it is important to consider the occurrence possibility among all three parameters for designing cooling systems more realistically. This study has used the Copula function method to establish muti-parameter joint distribution functions for internal disturbances, and expressed the possibility of simultaneous occurrence in the form of joint probability. By considering the unguaranteed rate of internal cooling load, this study obtained a trade-off result between two conflicting objectives including the maximum joint probability and the minimum unguaranteed rate. This method was justified to provide closer design values to actual situation than considering all parameters separately, which can replace the internal disturbances parameters recommended in the design standards for load calculations of new buildings after counting a large number of measured data in existing buildings with the same type.

The rest of the paper will introduce the new method developed for analyzing the joint probability of muti-parameters in terms of internal disturbances and methods for validation of results in Section 2, with the steps of trade-off optimization presented. Section 3 will describe the two case study buildings used in this study and the measured results from them. These results will be used in Section 4 to establish the joint probability distribution functions of cooling load disturbances. The main findings from this study will be summarized in the conclusion section of this paper.

2. Methodology

To optimize the quantification of design parameters considering combining their extreme conditions and maximum joint probabilities, a trade-off approach has been proposed in this study, with a research framework depicted in Figure 1.
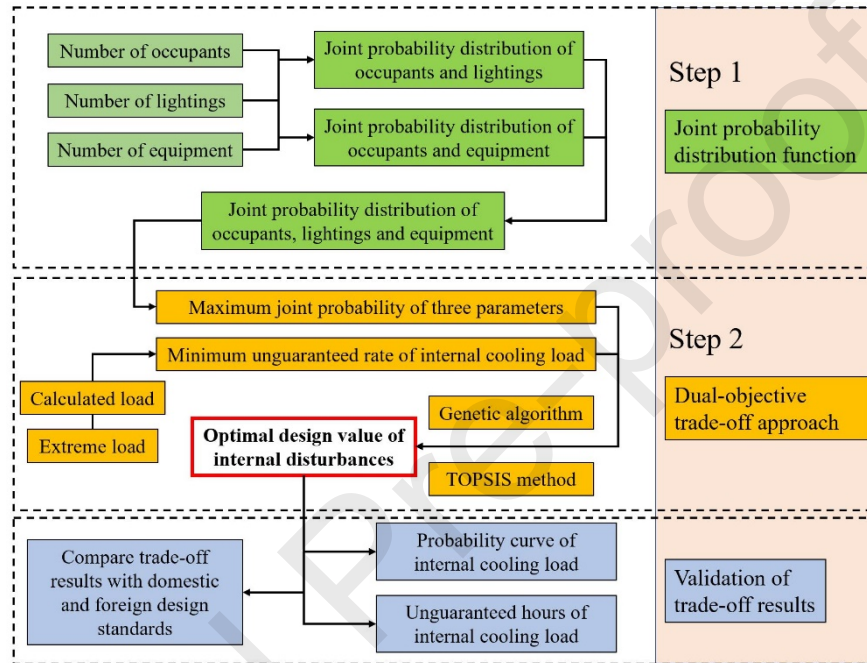

Figure 1: Proposed research framework

The trade-off approach can be specifically divided into the following two steps:

Step 1: Establishing joint probability distribution functions for internal disturbances including occupancy, lighting and equipment, to describe their joint occurrence probabilities;

Step 2: Deciding trade-offs using a combination of dual-object optimization method and TOPSIS decision method.

2.1 Step 1: establishing joint probability distribution functions

According to building design standards [38, 49, 50, 51], there are three major internal

disturbances, namely, occupancy density, lighting power density and equipment power density, when deciding the cooling load of a building. Additionally, their maximum values are usually used to cover extreme conditions. In real buildings, however, the probability of a single parameter reaching its extreme value is small, nevertheless when all three parameters reaching their extreme values simultaneously. Therefore, to design cooling systems more realistically, it is important to consider the occurrence possibility among all three parameters. In the statistical domain, Copula theory is a method of multivariate analysis. Using this method, multivariate joint distribution functions can be decomposed into a marginal distribution function to describe the probability distribution of a single parameter and a Copula function [38]. Using the Copula function, the correlation between random variables and their marginal distributions can be analyzed separately. Tahir et al. [39] used the best-fit copula estimate to define the degree of correlation between the percentage load and the converter efficiency. Huang et al. [40] used copula joint distribution function to describe the relationship between vegetation and groundwater depth and estimate the conditional probability of achieving ecological protection target. Therefore, it can describe the correlations among occupants, lighting and equipment, respectively, hence establishing marginal distribution functions of these three parameters and a three-parameter distribution function for calculating the joint probability of internal disturbances.
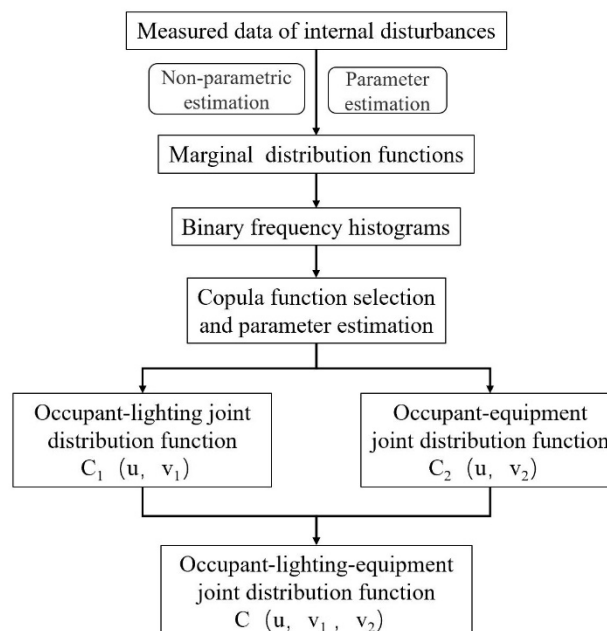
Figure 2: The construction process of joint distribution functions

In this study, Matlab, a popular computational tool for numerical calculation [40], has been used to construct the Copula function. Based on measured behavioral data from real buildings, the marginal distribution of the single parameters could be calculated. The kernel density estimation method is used to analyze the measured data based on the Gaussian kernel function and six probability distributions are fitted to the measured data. Then the fitting errors of the probability distributions are calculated respectively for determining the type of distribution functions by Equation 1,

$$Err = \frac{1}{n}\sum_{i=1}^{n}\left|\frac{x_i - t_i}{x_i} \times 100\%\right| \qquad (1)$$

where x_i is the measured values, dimensionless; t_i is the estimated values, dimensionless.

Besides, the binary frequency histograms could be established for both occupant-lighting and occupant-equipment. Then suitable Copula functions were selected by analyzing the tail correlation and symmetry between the parameters to describe the correlations both between any two parameters and among the three parameters, and the maximum likelihood estimation method was then used to calculate the values of the parameters in the functions. This construction process has been depicted in Figure 2.

2.2 Step 2: deciding trade-offs using the TOPSIS decision method

The internal cooling load can rarely reach its maximum value in real conditions, but it is still important to meet extreme load requirements in the cooling load calculation. However, pursuing only the satisfaction of the extreme load and ignoring the possibility of the event may cause unnecessary waste of energy from the cooling system. In this procedure, there are two conflicting objectives, i.e. maximum joint probability and minimum unguaranteed rate. The former objective means that the internal cooling load

calculated from internal disturbances with maximum joint probability is close to the actual situation. On the contrary, the latter objective means that the calculated internal cooling load is given to approach the ideal extreme conditions, which is far from the actual situation.

To establish a benchmark for the trade-off approach which is aim to find a compromised solution between two conflicting objectives, the deviation of the calculated internal cooling load from the design internal cooling load under extreme conditions was evaluated. Therefore, an unguaranteed rate (P) has been proposed as one of the trade-off targets, and this parameter was defined as the difference between the calculated internal cooling load and the design internal cooling load under extreme conditions, as defined by Equation 2,

$$P = \frac{Q_{\mathrm{D}} - Q_{\mathrm{C}}}{Q_{\mathrm{D}}} \times 100\% \tag{2}$$

where Q_{D} is the design internal cooling load under extreme conditions, in kW, and Q_{C} is the calculated internal cooling load under extreme conditions, in kW.

The internal cooling load (Q_{in}) is mainly due to indoor heat sources, mainly including occupants, lighting and equipment, as defined by Equation 3, and the heat loss due to insulation or leakage is not considered in this study.

$$Q_{in} = Q_P + Q_L + Q_E \tag{3}$$

where Q_{in} is the internal cooling load of a building, in kW; Q_P is the internal heat gain from occupants, in kW; Q_L is the internal heat gain from lighting, in kW, and Q_E is the internal heat gain from equipment, in kW.

The internal heat gain from occupants can be decided by Equation 4,

$$Q_P = qn \tag{4}$$

where q is the heat gain from one single occupant, in kW, and n is the total number

of occupants in the building, dimensionless.

The internal heat gain from lighting can be decided by Equation 5,

$$Q_L = n_1 P_1 X_{1t} + n_2 P_2 X_{2t} + \cdots + n_i P_i X_{it} \tag{5}$$

where i is the type of lighting, dimensionless; n_i is the number of lighting for type i, dimensionless; P_i is the power of lighting for type i, in kW, and X_{it} is the operational state of lighting at time t, with 0 for off and 1 for on, dimensionless.

The internal heat gain from equipment can be decided by Equation 6,

$$Q_E = n_1 P_1 X_{1t} + n_2 P_2 X_{2t} + \cdots + n_i P_i X_{it} \tag{6}$$

where i is the type of equipment, dimensionless; n_i is the number of equipment for type i, dimensionless; P_i is the power of equipment for type i, in kW, and X_{it} is the operational state of equipment at time t, with 1 for on, 0.3 for standby and 0 for off, respectively, dimensionless [41].

Evolutionary algorithms have been widely used in optimization problems due to their robustness and flexibility in yielding solutions in complex applications, which can be modified to adapt to multi-objective optimization using the Pareto front approach [42]. The non-dominated sorting genetic algorithm [43] is one technique suitable for optimizing multi-objective problems with two or three objective functions [44]. To balance the two objectives considered in this study, the genetic algorithm has been applied to seek feasible solutions from dual-objective optimization, in which a couple of optimal non-dominating points were given on the Pareto front, and then the multicriteria decision-making tool was used to find the final optimal solution [45]. The TOPSIS method was applied to select the optimal design solution from the Pareto fronts, which basic principle is to calculate the closeness degree based on the Euclidean distance from the evaluation scheme to the positive and negative ideal solutions, and then the schemes are ranked according to the closeness degree. [46]. The detailed steps

are as followings:

(1) The optimization objective function is constructed in terms of both the maximum joint probability and the minimum unguaranteed rate. It is then used to maximize the joint probability of the selected internal disturbances, which is calculated by the three-parameter joint probability function. Meanwhile, the unguaranteed rate is to minimize the difference between the calculated load and the extreme load.

(2) Running the genetic algorithm in Matlab to generate a Pareto front curve based on the non-dominated solution. The settings of relevant parameters for the optimization are listed in Table 2.

Table 2: The parameters settings of genetic algorithm

Initial population size	50
Maximum number of iterations	500
Crossover probability	0.6
Mutation probability	0.06

(3) The TOPSIS decision making method is used to evaluate the different design solutions on the Pareto front curve, and it can be divided into following steps [47]:

Assuming that the dual-objective decision-making matrix $(X_{ij})_{2 \times t}$ is composed of t evaluation indicators and two solutions, it can be expressed by Equation 7,

$$(X_{ij})_{2 \times t} = \begin{bmatrix} X_{11} & X_{12} & \cdots X_{1t} \\ X_{21} & X_{22} & \cdots X_{2t} \end{bmatrix} \tag{7}$$

where x_{ij} is the eigenvalue of indicator j in the solution i.

The distance scale is used to measure sample gap, which requires isotropy for different

indicator attributes. The transformation process can be expressed as Equation 8,

$$x'_{ij} = \frac{1}{x_{ij}} \tag{8}$$

In TOPSIS, a weight is needed for each indicator [48], so the entropy weight method was used to weight each indicator, given by Equations 9-21.

The standardization of the indicators of various solutions was calculated by Equation 9,

$$k_{ij} = \frac{x'_{ij} - \min(x'_j)}{\max(x'_j) - \min(x'_j)} \tag{9}$$

The specific weight of each indicator was expressed by Equation 10,

$$P_{ij} = \frac{k_{ij}}{\sum_{i=1}^{s} k_{ij}} \tag{10}$$

The Entropy value of each indicator was expressed by Equation 11 and Equation 12,

$$E_j = -m\sum_{i=1}^{s} P_{ij} \cdot \ln P_{ij} \tag{11}$$

$$m = \frac{1}{\ln s} \tag{12}$$

The Entropy weight of each indicator was expressed by Equation 13,

$$W_j = \frac{1 - E_j}{\sum_{j=1}^{t}(1 - E_j)} \tag{13}$$

The isotropic normalization of the data was expressed by Equation 14,

$$U_{ij} = \begin{cases} \dfrac{x_{ij}}{\sum_{i=1}^{s}(x_{ij})^2} \\ \dfrac{x'_{ij}}{\sum_{i=1}^{s}(x'_{ij})^2} \end{cases} \tag{14}$$

The construction of the normalized weighting matrix was expressed by Equation 15 and Equation 16,

$$Z = \begin{bmatrix} Z_{11} & Z_{11} & \cdots & Z_{1t} \\ Z_{21} & Z_{22} & \cdots & Z_{2t} \\ \vdots & \vdots & \vdots & \vdots \\ Z_{s1} & Z_{s2} & \cdots & Z_{st} \end{bmatrix} \qquad (15)$$

$$Z_{ij} = W_j U_{ij} (i = 1,2...,s; j = 1,2,...t) \qquad (16)$$

The selection of the optimal solution Z^+ and the worst solution Z^- was expressed by Equation 17 and Equation 18,

$$Z^+ = \{\max Z_{i1}, \max Z_{i2}, ... \max Z_{is}\} \qquad (17)$$

$$Z^- = \{\max Z_{i1}, \max Z_{i2}, ... \max Z_{is}\} \qquad (18)$$

The calculation of the distances between the evaluation unit and the optimal/worst solutions was expressed as Equation 19/20,

$$D_i^+ = \sqrt{\sum_{i=1}^s (\max Z_{ij} - Z_{ij})^2} \qquad (19)$$

$$D_i^- = \sqrt{\sum_{i=1}^s (\min Z_{ij} - Z_{ij})^2} \qquad (20)$$

The calculation of the relative closeness was expressed as Equation 21,

$$C_i = \frac{D_i^-}{D_i^+ + D_i^-}$$

(21)

All solutions could be ranked and evaluated based on the relative closeness C_i, with the best compromising solution with the largest value.

2.3 Compare and validate trade-off results with reference parameters in existing design standards

After deciding trade-offs between two objectives, the probability curve and unguaranteed hours of internal cooling load are used to validate trade-off results. The

Monte Carlo method, which can use a series of random numbers to model stochastic processes [49], has been used for random sampling of internal disturbances for cooling load simulation to obtain the probability distributions of different internal cooling load and the cumulative probability curve, which can be used to compare the internal cooling load calculated from the trade-off results with that under extreme and maximum probability cases. Then the unguaranteed hours of internal cooling load are calculated based on the cooling hours to further justify the optimal solutions selected by the trade-off approach.

The recommended values of the internal disturbance in the design standards of three countries are selected for comparison with the trade-off results, and the parameters of internal disturbances are multiplied with the hourly operation schedules for occupancy rate, lighting usage rate and equipment usage rate to obtain the internal disturbances schedules for hourly occupancy density, lighting power density and equipment power density using the Chinese energy-saving design standard as an example. Then it is compared with the measured data to verify the rationality of the trade-off results. Besides, the DesignBuilder is used to perform energy simulation calculations to illustrate the energy efficiency benefits of the trade-off approach to building energy consumption. Two office buildings are modeled in DesignBuilder software, and the envelope parameters, occupancy, operation schedules of lighting and HVAC systems are defined based on the collected information. Referring to ASHRAE Handbook [50], the models are calibrated in terms of meteorological parameters, envelope parameters, schedules, internal loads, and system operation based on the energy-saving design standard and measured data. And then the normalized mean bias error (NMBE) and the coefficient of variance of the root mean square error [CV(RMSE)] are used to validate the building models, as defined by Equation 22 and 23,

$$NMBE = \frac{\sum(V_{actual} - V_{modeled})}{(N-1) \times Mean(V_{actual})} \times 100\% \qquad (22)$$

14

$$CV(RMSE) = \frac{\sqrt{\frac{\Sigma(V_{actual} - V_{modeled})^2}{N-1}}}{Mean(V_{actual})} \times 100\% \qquad (23)$$

where V_{actual} is parameter's measured or metered value for each time step, $V_{modeled}$ is parameter's estimated or modeled value for each time step, and N is number of time steps being analyzed during period of evaluation.

It is suggested that a building model is considered accurate if the $NMBE$ is within 5% and the $CV(RMSE)$ is below 15% when monthly data are used [50].

3. Case study

3.1 Data acquisition

An academic office building (Office Building A) and a business office building (Office Building B), both located in Tianjin, China, have been selected in this study, as shown in Figure 3. Building A has about 70% of rooms being either single or multi-person offices, with a total floor area of 3,690 m² and an opening time from 6:00am to 11:00pm. Building B has a total floor area of 10,238 m² and an opening time from 8:30am to 5:30pm, with various functional types of rooms including offices, meeting rooms and event rooms. For both building, there are no nearby objects, such as other buildings and tall trees. Therefore, there is no shading effect on their cooling loads.
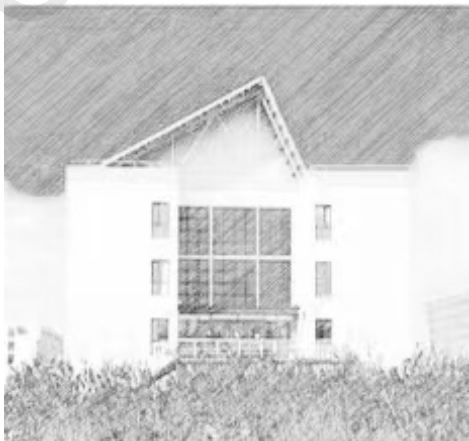
Figure 3: Pictures of the academic office building (left) and business office building (right)

The occupants' behavior related data in the buildings include the room occupancy and power density of lightings and equipment. A combination of physical monitoring and questionnaires was selected in this study. The specific test subjects and contents are shown in Figure 4.
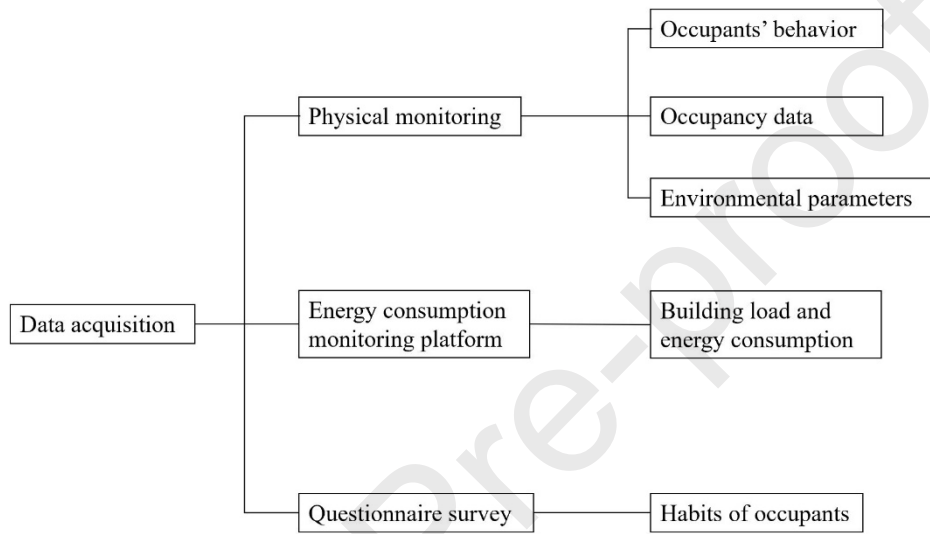

Figure 4: Test contents and methods

By using passive infrared sensors and cameras for occupancy detection and behavior recording, physical monitoring concentrates on the data of indoor environmental parameters, occupancy data and the equipment usage data [51]. Questionnaire survey allows direct understanding of personal motivations of various behaviors [52] and thoughts of controlling devices in a multi-person environment in a non-invasive way [53].

A two-month field test was conducted from July to August 2020. The historical data such as hourly cooling load and sub-electricity consumption in the past five years was collected from the energy monitoring platforms in both of the office buildings. It was found that the total number of occupants in the buildings has not changed much in size

over the past five years, which shows that both buildings have been in stable operation in recent years. Therefore, the data obtained from the two-month test in summer is representative enough for the verification of the proposed method for seeking the design parameters of internal cooling load. The specific testing scheme is listed in Table 3 and the questionnaire is shown in Appendix A.

Table 3: Test parameters and equipment

Test parameters	Test equipment	Equipment accuracy	Equipment location	Test interval
Indoor temperature and humidity	Self-recording temperature and humidity meter	± 0.8%/± 5%	Desk side	5 min
Working surface illumination	Self-recording illuminance meter	± 5%	Unobstructed working surface area	5 min
Lighting status	Cameras	360° horizontal and 180° vertical viewing angle	Unobstructed desktop	1 h
Window status	Window magnetic sensor	± 0.1%	Windows	5 min
Computer power	Intelligent power socket	± 2%	Computer sockets	1 h

3.2 Characteristics analysis of test data

The occupants are the main user of the buildings, and the occupancy rate is the most important factor influencing the variation of the building cooling load. The design numbers and hourly numbers of occupants in the office buildings are counted as shown in Figure 5.
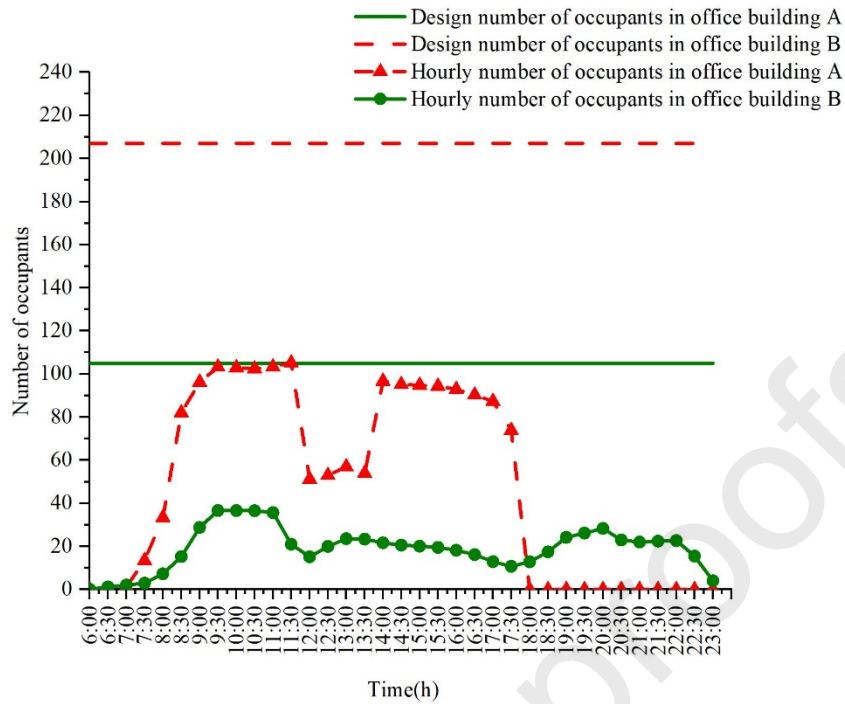
17

Figure 5: Design and hourly numbers of occupants in two office buildings

It can be seen that the design numbers of occupants in the buildings far exceed the actual maximum numbers. In office building A, the hourly number of occupants shows a "three-peak distribution" as a whole, while in office building B, the hourly number of occupants shows a "two-peak distribution". The number of occupants fluctuates in a wide range which varies with great randomness, and the mobility of occupants is the greatest during meal and commuting hours. From the occupancy rate data of two office buildings, it can be seen that the occupancy density recommended in the design manual [41] is seriously deviate from the actual situation in existing office buildings. The actual occupancy rate is only about 60% of the original design profiles or even lower during most of the time.

The cameras are used in two office buildings for real-time monitoring of lighting behavior and the number of lights turned on in the room. Then the lighting power density is calculated from the number of running lightings and the power, as show in Figure 6.
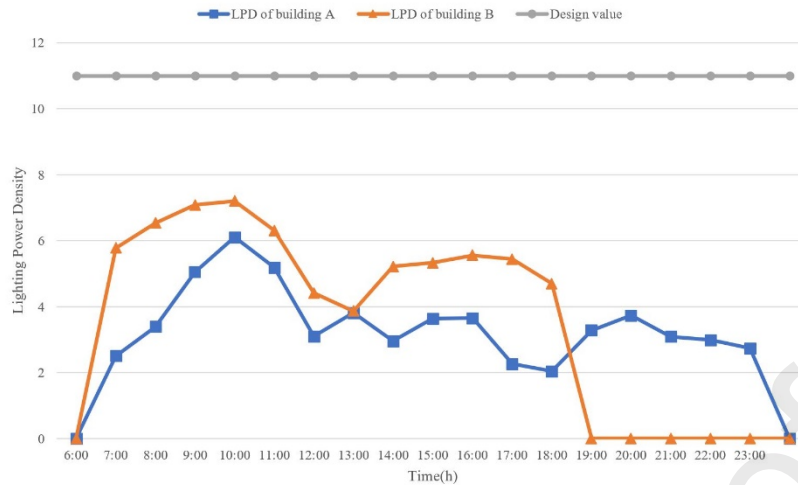
Figure 6: Hourly lighting power density in two office buildings

In Figure 6, the hourly lighting power density in office building B shows a "two-peak distribution", while it shows a "three-peak distribution" in office building A. Most of the occupants will enter the building gradually from 7:30 and choose to turn on the light according to their own lighting using habit or energy saving consciousness. The number of lights decreases during the midday hours due to the absence of occupants or the increase of outdoor light intensity. Due to the different job and lighting using habits of occupants in the two buildings, the lighting power densities are also different. But it can be seen that the maximum lighting power densities of the two buildings are still lower than the design value.

The most frequently used equipment in office buildings with the largest heat gain is the computer, so only the mode and proportion of running computers in the buildings are focused in this study. Then the computer power density is calculated from the number of running computers and the power. Due to the design work with a high frequency of using computers of occupants in office building A, the monitoring data of the number of running computers in office building A is analyzed as an example. The computer usage patterns can be divided into three modes including running all day, off at noon and randomly running, with the number of occupants accounting for 60%, 27% and 13% respectively.
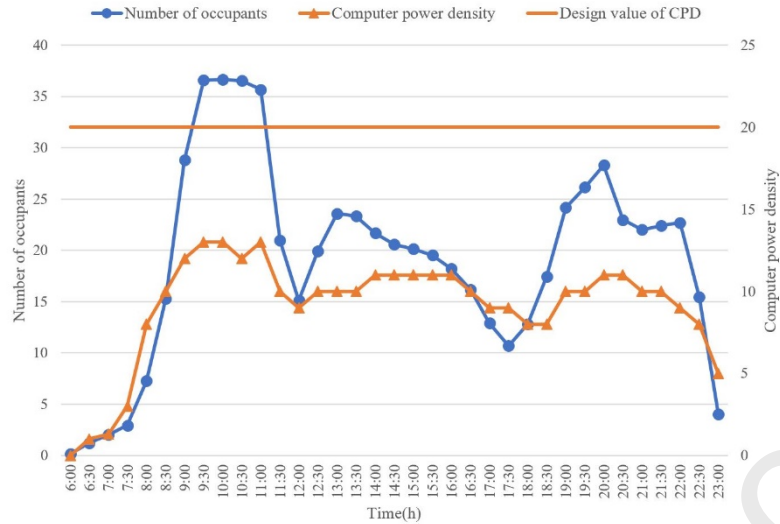
Figure 7: Hourly changes in the computer power density and numbers of occupants

It can be seen that the overall trends of the number of running computers and occupants are consistent, which have a fluctuation pattern in a small range except for a certain decrease during lunch time. But the computer power density is much lower than the design value.

4. Results and discussion

4.1 Marginal distribution functions of internal disturbances

The probability density distributions of the single parameters are calculated using MATLAB based on the kernel function, and the least squares method is used to fit the measured data. The fitted curves of the six probability distributions are compared with the statistical results of measured data as shown in Figure 8.
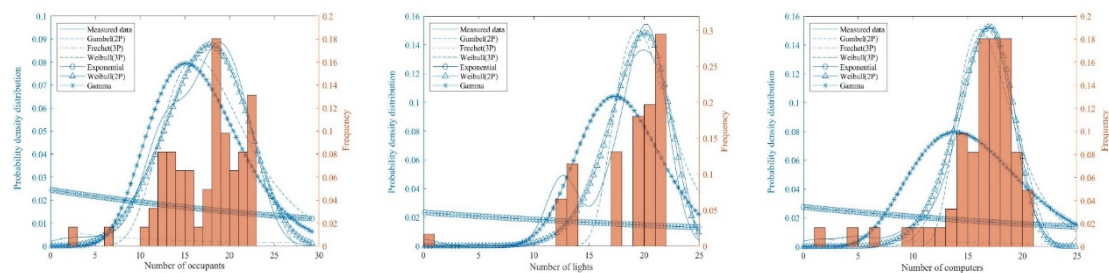
Figure 8: Probability density distribution of three single parameters

The fitting errors are calculated using the method mentioned in Section 2.1, and the one with the minimum cumulative fitting error of the probability density distributions of three single parameters is the Weibull distribution, so the Weibull distributions are used in this paper to describe the probability distribution of room occupancy, lighting usage and equipment usage respectively.

4.2 Joint probability distribution of internal disturbances

4.2.1 Room occupancy and lighting usage

Figure 9 shows a binary frequency histogram for the occupancy rate and the proportion of lighting usage, built upon the measured data from the study. The tail variation characteristics have been analyzed to select a suitable joint distribution function between room occupancy and lighting usage.
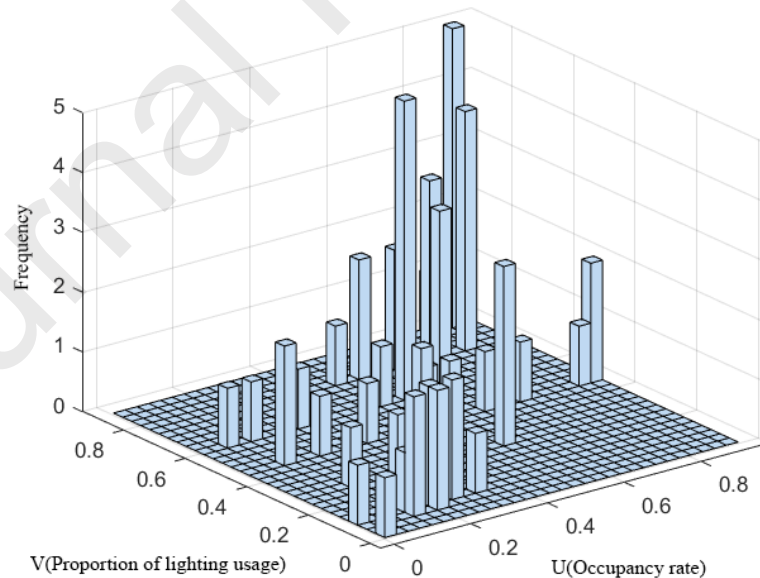

Figure 9: Binary frequency histogram of occupancy rate and proportion of lighting usage

It can be seen that the occupancy rate and the proportion of lighting usage have

symmetrical tails, indicating that a high correlation between the two parameters. A binary normal Copula function was selected according to the tail independence and the parameter values were calculated using the maximum likelihood estimation method. Figure 10 shows the probability density distribution and the joint distribution of the two parameters, with the occupancy rate mainly concentrated between 60% and 80% and the proportion of lighting usage mainly concentrated between 60% and 70%.
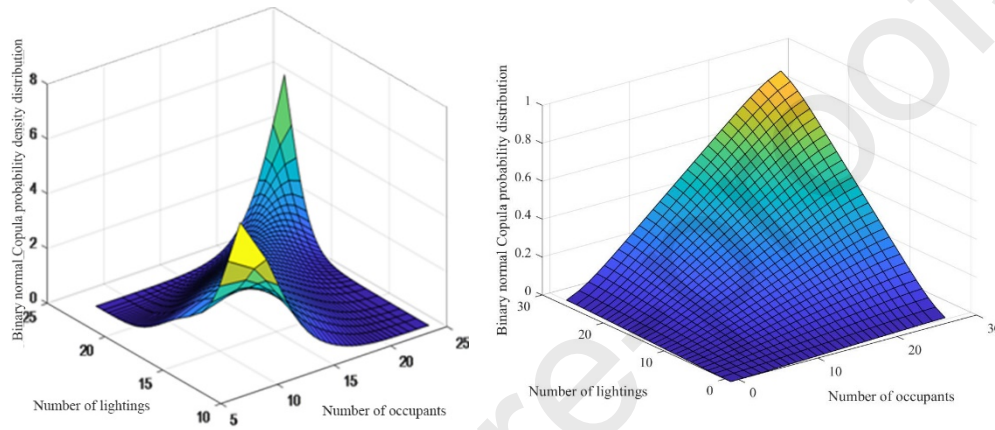

Figure 10: Probability density distribution and joint distribution of the binary normal Copula function

The binary normal Copula function between the occupancy rate and the lighting usage can be defined by Equation 24,

$$C^G(u;v) = \int_{-\infty}^{\phi^{-1}(u)} \int_{-\infty}^{\phi^{-1}(v)} \frac{1}{2\pi\sqrt{1-0.7331^2}} \exp\left[-\frac{s^2 - 2 \times 0.7331st + t^2}{2(1-0.7331^2)}\right] dsdt \qquad (24)$$

4.2.2 Room occupancy and equipment usage

Figure 11 shows the binary frequency histogram for the occupancy rate and the proportion of computer usage, also obtained from the measured data, with the tail variation characteristics analyzed for selecting a suitable joint distribution function to describe the joint probability distribution characteristics.
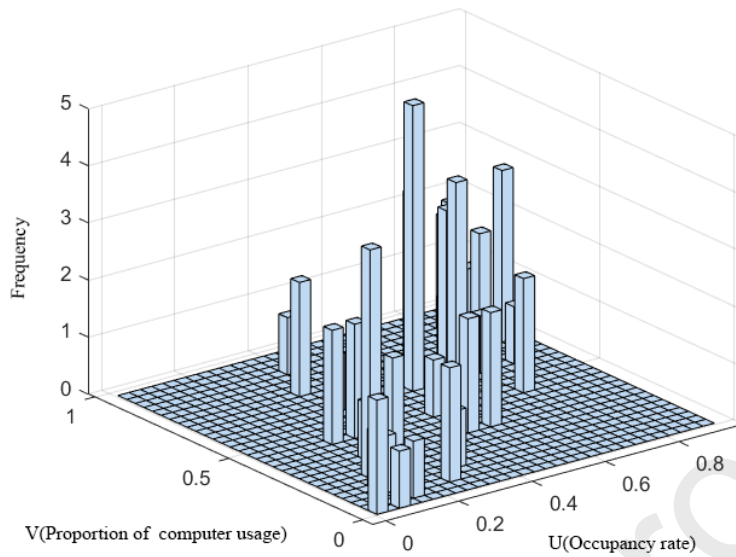
Figure 11: Binary frequency histogram of occupancy rate and proportion of computer usage

It can be seen that the occupancy rate and the proportion of computer usage have symmetrical tails, so a binary normal Copula function was selected according to the tail independence and the parameters were calculated using the maximum likelihood estimation method. Figure 12 shows the probability density distribution and the joint distribution of both parameters. The occupancy rate was mainly concentrated between 60% and 80%, and the proportion of computer usage was between 50% and 70%.
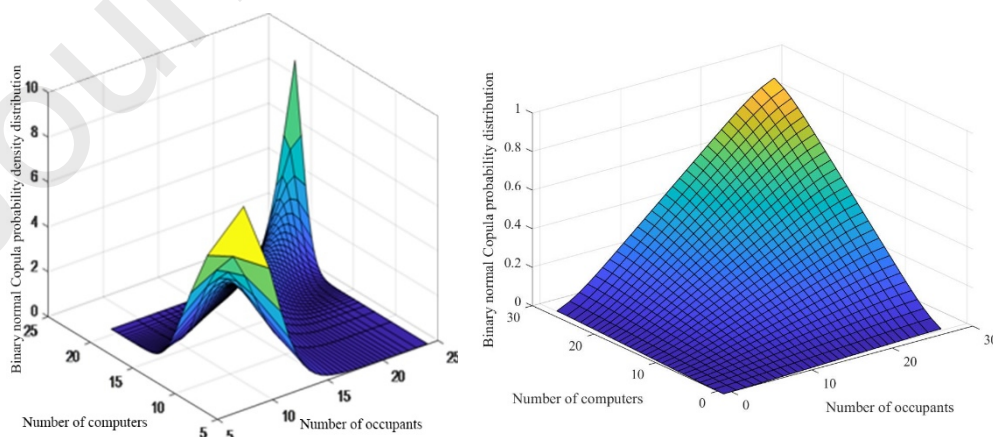

Figure 12: Probability density distribution and joint distribution of the binary normal Copula function

The binary normal Copula function of the occupancy rate and the computer usage can be defined by Equation 25,

$$C^G(u;v) = \int_{-\infty}^{\phi^{-1}(u)} \int_{-\infty}^{\phi^{-1}(v)} \frac{1}{2\pi\sqrt{1-0.854^2}} \exp\left[-\frac{s^2 - 2\times 0.854st + t^2}{2(1-0.854^2)}\right] dsdt \qquad (25)$$

4.2.3 Room occupancy, lighting usage and equipment usage

The dual-parameter joint probability functions were used as the marginal distribution functions to construct the three-parameter joint probability distribution function, and the Clayton Copula function was selected due to the asymmetry of the marginal distribution whose parameter values were calculated using the maximum likelihood estimation method. The joint distribution function of the three parameters were defined by Equation 26,

$$C_3(u,v_1,v_2) = \left(C_1\left(u,v_1\right)^{-\theta} + C_2(u,v_2)^{-\theta} - 1\right)^{-\frac{1}{\theta}}, \quad \theta = 3.12$$
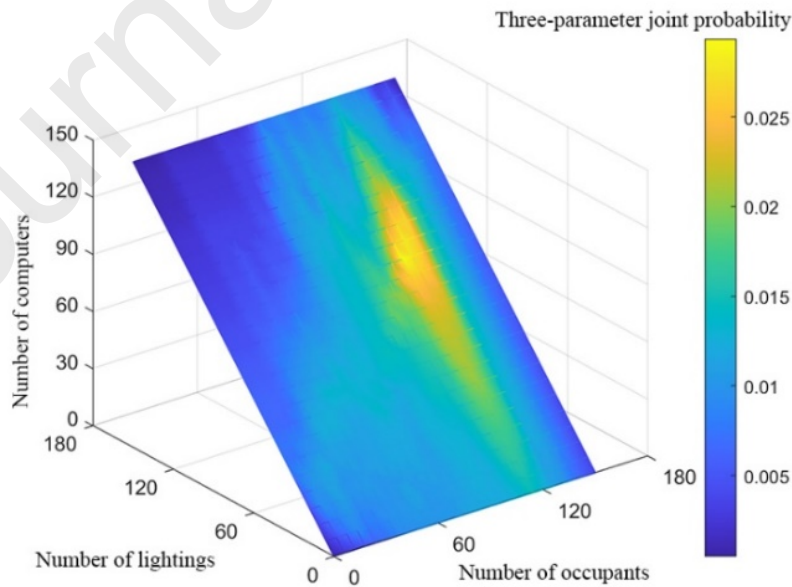
(26)

Figure 13: Three-parameter joint probability distribution

Figure 13 shows the joint probability distribution of three parameters. It can be seen that when the occupancy rate lies in between 60% and 80%, the joint distribution probability is the largest; and when the number of occupants reaches the maximum, the joint probability is very small, and the probability that all three parameters reach the extreme values at the same time is almost zero. Besides, the probability of lighting usage and computer usage increased with the number of occupants, which is consistent with the trend of room occupancy, lighting usage and computer usage shown in Section 3.

4.3 Optimal solution selection

In this study, the genetic algorithm was used to optimize the two objectives, i.e. the maximum three-parameter joint probability and minimum unguaranteed rate of internal cooling load, with the optimal solution of Pareto front obtained shown in Figure 14.
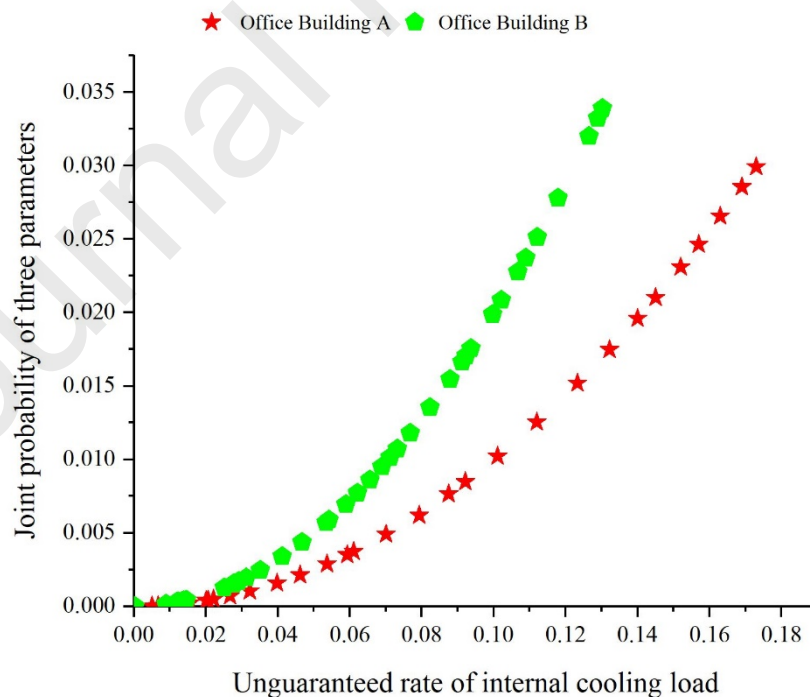

Figure 14: Pareto optimal solutions

A higher joint probability of the internal disturbances indicates a more rational solution, while it is opposite for the unguaranteed rate of the internal cooling load. Therefore, in the indicator convergence process, the inverse of the unguaranteed rate needs to be used. According to Equation 9-21, the weight of each index was calculated using the entropy weight method based on the dimensionless standardization of each index, with a bigger weight indicating a greater influence on the evaluation of the solutions.

To decide the optimal and worst solutions, the normalized weighted decision matrix was obtained by weighting the weight matrix and the normalization matrix, with results listed in Table 4.

Table 4: The positive and negative ideal solutions of two office buildings

	Solution	Unguaranteed rate of internal cooling load	Joint probability of internal disturbances
Office building A	Z^+	1.112	3.528
	Z^-	3.987	0.001
Office building B	Z^+	1.023	5.621
	Z^-	4.412	0.667

The optimal design parameters were selected by calculating the relative proximity based on the distance from the positive and negative ideal solutions of each solution, and Table 5 lists the optimal results from the Pareto front.

Table 5: Optimal solutions of the two office buildings

Occupancy density (Person/m²)	Lighting power density (W/ m²）	Computer power density (W/ m²）	Unguaranteed rate	Joint probability

26

| Office building A | 0.08 | 4.97 | 13.24 | 15.20% | 2.31% |
| Office building B | 0.10 | 6.37 | 14.89 | 10.67% | 2.28% |

4.4 Optimal solution validation

To further validate the optimal solutions selected by the trade-off approach, the probability curve and the unguaranteed hours of internal cooling load were used, compared to that in both extreme and maximum probability cases.

4.4.1 The probability curve of building internal cooling load

The Monte Carlo method was used for random sampling of internal disturbances to simulate cooling load. Figure 15 shows the probability distribution of internal cooling load, with Points A and C indicate the design values of internal cooling load in the existing standard and the value under maximum probability, respectively. Point B is the design value derived from this study.
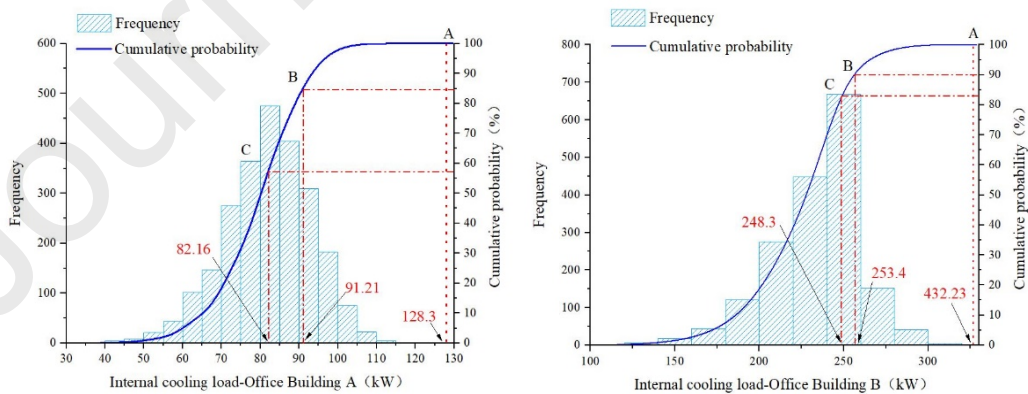

Figure 15: Probability distribution of internal cooling load of two office buildings

From the result, it can be seen that for Office building A and Office building B, the calculated design internal cooling load according to the standard manual was 128.30kW

and 432.23kW respectively, exceeding the peak cooling load by 11.56% and 33% respectively. Additionally, the cumulative probability of the cooling load at Point A had reached 100%, further indicating that the calculated cooling load according to the standard manual had far exceeded the actual cooling load. For Point B, however, the obtained design values still ensured the cooling load demand of the buildings during most of the operating hours, even these values were lower than the standard values. Additionally, Point B was located at the inflection point of the cumulative probability curve. On its left side, a slight decrease in the design parameters of internal cooling load would cause a significant increase in the unguaranteed rate of internal cooling load. On its right side, even if a significance increase in internal disturbances would not reduce unguaranteed rate greatly. Therefore, the rationality of setting point B with appropriate values of internal disturbances as the design point is verified.

4.4.2 The unguaranteed hours of internal cooling load

The unguaranteed hours of internal cooling load reflect the unguaranteed situation under the condition of extreme values of internal disturbances. Figure 16 shows the results of unguaranteed hours under different unguaranteed rates.
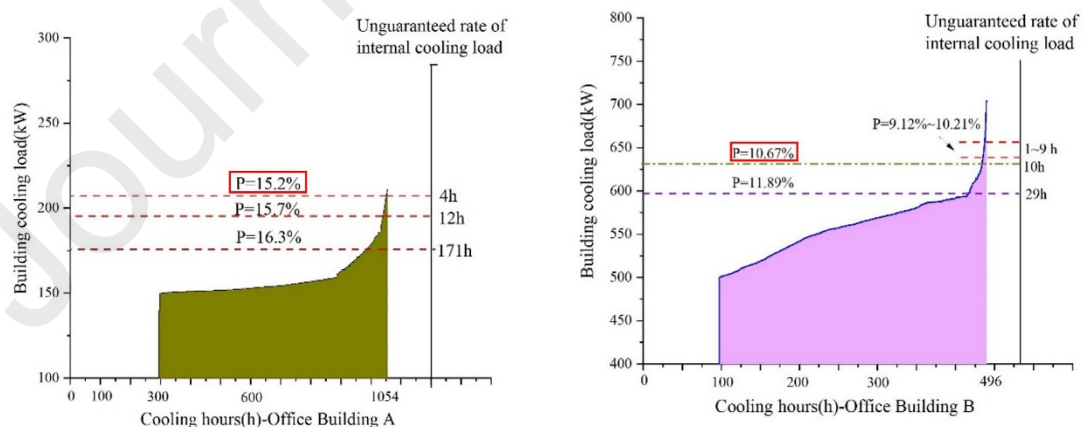

Figure 16: Unguaranteed hours under different unguaranteed rates of two office buildings

For Office building A, it can be seen that when the unguaranteed rate of internal cooling

load increased from 15.2% to 15.7%, the unguaranteed hours during the operation hours increased from 4 hours to 12 hours. When the unguaranteed rate of internal cooling load continued to increase to 16.3%, the number of unguaranteed hours increased sharply by nearly 42 times, i.e. from the 4 unguaranteed hours to 171 unguaranteed hours, the occupancy density remained at 0.18 person/m^2, the lighting power density was reduced by 0.36W/m^2 only, and the equipment power density was reduced by 0.38 W/m^2 only. It can be seen that a small decrease of internal disturbances would significantly increase the number of unguaranteed hours. For Office building B, it can also be seen that when the unguaranteed rate of internal cooling load increased from 10.67% to 11.89%, the unguaranteed hours during the operation hours increased nearly three times. Besides, Therefore, the optimal design solution is able to satisfy the unguaranteed hours with lower values for internal disturbances.

4.5 Design value comparison

The TOPSIS method was used to determine the optimum design solution of internal disturbances, which balances the joint probability and the unguaranteed rate. The trade-off results were compared with the values given in major building design standards, as shown in Table 6.

Table 6: Comparison of internal disturbances

	Building type	Occupancy density （Person/m^2）	Lighting power density （W/m^2）	Equipment power density （W/m^2）
Design standard of GB 55015-2021 [54]	Office	0.10	8	15
ASHRAE standard 90.1 [55]	Office	0.05	10.76	15
DIN V 18599 2018 [56]	Office	0.1	13	15
Office building A	Office	0.08	**4.97**	13.24

| Office building B | Office | 0.10 | **6.37** | 14.89 |

It can be seen that the values in major building design standards are generally higher than the values given by the optimum design solution. Both the occupancy density and equipment power density in the optimum design solution were basically consistent with the energy-saving design standards, indicating that the selected parameters are in line with the standards, which verifies the effectiveness of the method. However, the difference of the lighting power density between the optimum design solution and design standards is large, mainly because of the lower proportion of running lightings during most of the operating hours even when the occupancy rate is high. Therefore, it is recommended that the lighting power density used for cooling load calculations of office buildings in the design standards should be slightly reduced.
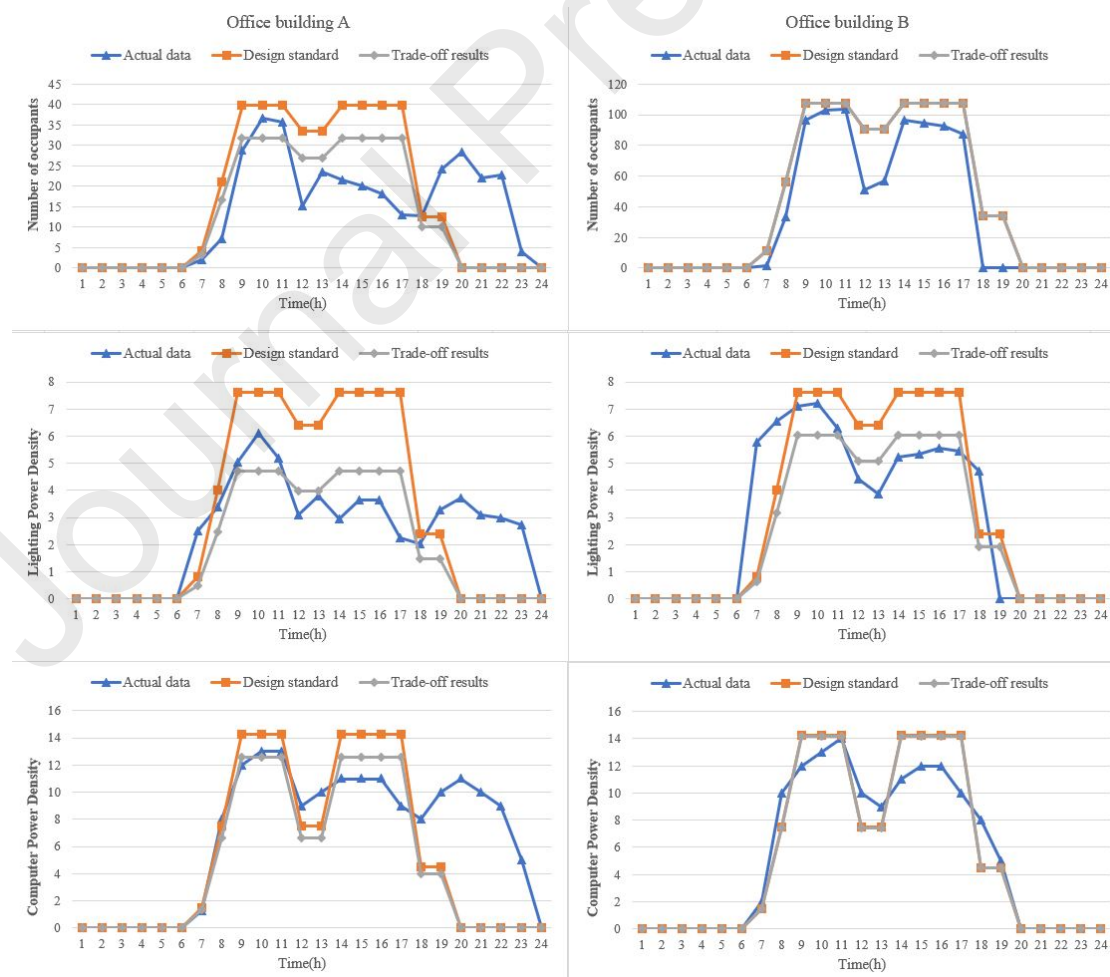
Figure 17: Comparison of schedules for internal disturbances calculated from the design
standard and trade-off results with actual data

Schedule is also an important parameter in cooling load design calculations. The
schedules for internal disturbances including number of occupants, lighting power
density and equipment power density calculated from the design standards [54] and
trade-off results were compared to the test data in Section 3. The results are shown in
Figure 17. It can be seen that the operating schedules calculated from the trade-off
results were closer to the actual test data in Office building A, except for the special
overtime situation at night which is not considered in the design standard. The same
results can be obtained in Office building B.

The values of internal disturbances were then substituted into DesignBuilder, a popular
dynamic building performance package [60], to calculate and compare the energy
consumption of a whole year, using Office buildings A and B. The definitions of
building performance parameters are available in Appendix B, where the operating
schedules remain the same. After calibrating, the monthly energy consumption data of
a whole year are used for validation, and the validation results are shown in Table 7.
Both the NMBE and CV(RMSE) are within the range required by the standard, so the
building model is considered accurate.

Table 7: The validation results of two office buildings

Buildings	NMBE (%)	CV(RMSE) (%)
Office building A	-3.8	12.7
Office building B	4.2	14.3

Table 8: The calculation results of energy consumption in Office building A

Energy	Energy	Energy	Total energy

	consumption of lighting (kWh)	consumption of computer (kWh)	consumption of occupants (kWh)	consumption for internal disturbances (kWh)
Design standard of GB 55015-2021 [50]	130615.10	77289.66	21244.56	229149.36
ASHRAE standard 90.1 [51]	177763.40	77289.66	10627.21	265680.25
DIN V 18599 2018 [52]	210979.90	77289.66	25066.92	313336.47
Trade-off results of building A	91327.64	54796.58	19926.03	166050.25

Table 9: The calculation results of energy consumption in Office building B

	Energy consumption of lighting (kWh)	Energy consumption of computer (kWh)	Energy consumption of occupants (kWh)	Total energy consumption for internal disturbances (kWh)
Design standard of GB 55015-2021 [50]	410031.61	226041.60	62908.34	698981.55
ASHRAE standard 90.1 [51]	552134.49	226041.60	24067.30	802243.39

DIN V 18599 2018 [52]	667303.65	226041.60	60117.45	953462.70
Trade-off results of building B	326905.05	224629.58	62745.69	614280.32

The simulation results are shown in Table 8 and Table 9. It can be seen that the total energy consumption calculated from the trade-off results of Office building A was at least reduced by 27.5%, while that of Office building B was at least reduced by 12.1%, compared to the results calculated by the recommended values in the design standards.

The reduction of lighting power density, however, will have an important influence on indoor visual environment, so it is necessary to evaluate whether the values of illuminance meet the requirement of the design standards after reducing the lighting power density. The lighting power density and illuminance conversion formula can be obtained from the design standards, as shown in Equation 27,

$$LPD = \frac{Eav}{\eta_s uK} \qquad (27)$$

where LPD is the lighting power density, in W/m^2; Eav is the illuminance, in lx; η_s is luminous efficacy of a light source, dimensionless, with a value range between 80-140 [57]; u is the utilization factor, dimensionless, generally taken as 0.6 for offices [57], and K is the maintenance factor, dimensionless, generally taken as 0.8 for offices [57].

Table 10: Calculated lighting power density

	Building type	Illuminance (lx)	The range of LPD (W/m^2)

33

GB 50034-2013 [57]	Office	300-500	
ANSI/IESNA RP-1-04 [58]	Office	300-500	**4.46-13.02**
DIN 5035-1 [59]	Office	300-500	

Referring to the design standards of various countries, the illuminance level in offices need to be maintained between 300-500lx, which needs the lighting power density to be between 4.46 and 13.02 W/m^2, as shown in Table 10. Therefore, the lighting power density obtained from the trade-off results which is 4.97 and 6.37 W/m2 can meet the requirement of the design standards.

5. Conclusion

The uncertainty and correlation of the internal load disturbances is often ignored in the design cooling load calculations and always result in the oversized cooling system, the trade-off approach is proposed to explore the optimal design parameters for internal cooling load calculation based on the joint probability of internal disturbances. By taking two office buildings as examples, the effectiveness of the method is verified by comparing the results with the design standards. The following conclusions can be drawn from the results.

(1) The Copula function can express the joint probability distribution of internal disturbances. The optimal design parameters can be determined from a trade-off between the two objectives, i.e. minimum unguaranteed rate and maximum joint probability.

(2) The trade-off results have been validated based on the frequency characteristics and the unguaranteed hours of internal cooling load.

(3) The actual occupancy rate is only about 60% of the original design profiles, or even lower for most of the time. By comparing with the trade-off results, the values of internal disturbances in the design standards need to be lowered to meet the energy-saving development trend, especially for the lighting power density, which is at least 26% higher than the trade-off results.

(4) The calculated schedules for internal disturbances based on both the design standard and the trade-off results have been compared with the test data, and the comparison showed that the schedules of internal disturbances calculated from the trade-off results were closer to actual situation. Simulation by DesignBuilder showed that the energy consumption for internal disturbances can be reduced by at least 27.5% and 12.1%, respectively, when using the trade-off results.

Aiming at providing optimum design parameters for internal cooling load calculations, a trade-off approach has been proposed in this study. However, due to the significant variation in both climate and building type, the results cannot be directly used in other buildings, but this method can be applied in various types of buildings in different climate zones in future studies. Besides, when this approach is applied to more types of buildings, multiple sets of trade-off results of internal disturbances can be calculated, and then the statistical values of internal disturbances for a certain type of buildings that are closer to the actual conditions can be obtained, which can replace the recommended values in the design standards to be applied in the building load design calculations.

Acknowledgement

References

[1] Q. Wen, J. Hong, G. Liu, P. Xu, M. Tang, Z. Li, Regional efficiency disparities in China's construction sector: A combination of multiregional input–output and data envelopment analyses, Applied Energy, 257 (2020) 113964.

[2] China Building Energy Consumption and Carbon Emission Research Report 2021. China Association of Building Energy Efficiency.

[3] H. Chaouch, C. Çeken, S. Arı, Energy management of HVAC systems in smart buildings by using fuzzy logic and M2M communication, Journal of Building Engineering, 44 (2021) 102606.

[4] H. Jiang, R. Yao, S. Han, C. Du, W. Yu, S. Chen, B. Li, H. Yu, N. Li, J. Peng, B. Li, How do urban residents use energy for winter heating at home? A large-scale survey in the hot summer and cold winter climate zone in the Yangtze River region, Energy and Buildings, 223 (2020) 110131.

[5] G. Zheng, X. Li, Construction method for air cooling/heating process in HVAC system based on grade match between energy and load, International Journal of Refrigeration, 131 (2021) 10-19.

[6] C. Fan, Y. Ding, Cooling load prediction and optimal operation of HVAC systems using a multiple nonlinear regression model, Energy and Buildings, 197 (2019) 7-17.

[7] C. Fan, Y. Liao, G. Zhou, X. Zhou, Y. Ding, Improving cooling load prediction reliability for HVAC system using Monte-Carlo simulation to deal with uncertainties in input variables, Energy and Buildings, 226 (2020) 110372.

[8] L. Zhu, J. Zhang, Y. Gao, W. Tian, Z. Yan, X. Ye, Y. Sun, C. Wu, Uncertainty and sensitivity analysis of cooling and heating loads for building energy planning, Journal of Building Engineering, 45 (2022) 103440.

[9] F. Wang, H. Lin, W. Tu, Y. Wang, Y. Huang, Energy Modeling and Chillers Sizing of HVAC System for a Hotel Building, Procedia Engineering, 121 (2015) 1812-1818.

[10] R.F.F. Pontes, W.M. Yamauchi, E.K.G. Silva, Analysis of the effect of seasonal climate changes on cooling tower efficiency, and strategies for reducing cooling tower power consumption, Applied Thermal Engineering, 161 (2019) 114148.

[11] W. Gang, S. Wang, K. Shan, D. Gao, Impacts of cooling load calculation uncertainties on the design optimization of building cooling systems, Energy and

Buildings, 94   (2015) 1-9.

[12] Y. Sun, L. Gu, C.F.J. Wu, G. Augenbroe, Exploring HVAC system sizing under uncertainty, Energy and Buildings, 81   (2014) 243-252.

[13] D. Woradechjumroen, Y. Yu, H. Li, D. Yu, H. Yang, Analysis of HVAC system oversizing in commercial buildings through field measurements, Energy and Buildings, 69   (2014) 131-143.

[14] P. Huang, G. Huang, Y. Wang, HVAC system design under peak load prediction uncertainty using multiple-criterion decision making technique, Energy and Buildings, 91   (2015) 26-36.

[15] R. Liang, W. Ding, Y. Zandi, A. Rahimi, S. Pourkhorshidi, M.A. Khadimallah, Buildings' internal heat gains prediction using artificial intelligence methods, Energy and Buildings, 258   (2022) 111794.

[16] R. Li, J. Zhang, Real-time heat dissipation model of electronic equipment for determining the dynamic cooling demand of office buildings, Journal of Building Engineering, 45   (2022) 103465.

[17] S. Wei, P.W. Tien, J.K. Calautit, Y. Wu, R. Boukhanouf, Vision-based detection and prediction of equipment heat gains in commercial office buildings using a deep learning method, Applied Energy, 277   (2020) 115506.

[18] I. Beausoleil-Morrison, Learning the fundamentals of building performance simulation through an experiential teaching approach, Journal of Building Performance Simulation, 12 (3) (2019) 308-325.

[19] J. Chapman, P.-O. Siebers, D. Robinson, On the multi-agent stochastic simulation of occupants in buildings, Journal of Building Performance Simulation, 11 (5) (2018) 604-621.

[20] Z. Wang, Y. Ding, H. Deng, F. Yang, N. Zhu, An Occupant-Oriented Calculation Method of Building Interior Cooling Load Design, Sustainability, 10 (6) (2018) 1821.

[21] Z. Wang, T. Hong, M.A. Piette, Data fusion in predicting internal heat gains for office buildings through a deep learning approach, Applied Energy, 240   (2019) 386-398.

[22] R. Ward, R. Choudhary, Y. Heo, A. Rysanek, Exploring the impact of different parameterisations of occupant-related internal loads in building energy simulation, Energy and Buildings, 123   (2016) 92-105.

[23] L.C. Tagliabue, M. Manfren, A.L.C. Ciribini, E. De Angelis, Probabilistic behavioural modeling in building performance simulation—The Brescia eLUX lab, Energy and Buildings, 128   (2016) 119-131.

[24] Y. Ding, Z. Wang, W. Feng, C. Marnay, N. Zhou, Influence of occupancy-oriented interior cooling load on building cooling load design, Applied Thermal

Engineering, 96 (2016) 411-420.

[25] S. Norouziasl, A. Jafari, C. Wang, An agent-based simulation of occupancy schedule in office buildings, Building and Environment, 186 (2020) 107352.

[26] M. Payet, M. David, P. Lauret, M. Amayri, S. Ploix, F. Garde, Modelling of occupant behaviour in non-residential mixed-mode buildings: The distinctive features of tropical climates, Energy and Buildings, 259 (2022) 111895.

[27] M. Hu, F. Xiao, Quantifying uncertainty in the aggregate energy flexibility of high-rise residential building clusters considering stochastic occupancy and occupant behavior, Energy, 194 (2020) 116838.

[28] X. Zhou, D. Yan, T. Hong, X. Ren, Data analysis and stochastic modeling of lighting energy use in large office buildings in China, Energy and Buildings, 86 (2015) 275-287.

[29] K. Amasyali, N. El-Gohary, Building Lighting Energy Consumption Prediction for Supporting Energy Data Analytics, Procedia Engineering, 145 (2016) 511-517.

[30] O. Sarfraz, C.K. Bach, Experimental methodology and results for heat gains from various office equipment (ASHRAE RP-1742), Science and Technology for the Built Environment, 24 (4) (2018) 435-447.

[31] S. Wei, J. Calautit, Development of deep learning-based equipment heat load detection for energy demand estimation and investigation of the impact of illumination, International Journal of Energy Research, 45 (5) (2021) 7204-7221.

[32] Q. Zhang, D. Yan, J. An, T. Hong, W. Tian, K. Sun, Spatial distribution of internal heat gains: A probabilistic representation and evaluation of its influence on cooling equipment sizing in large office buildings, Energy and Buildings, 139 (2017) 407-416.

[33] W. Gang, S. Wang, F. Xiao, D.-c. Gao, Robust optimal design of building cooling systems considering cooling load uncertainty and equipment reliability, Applied Energy, 159 (2015) 265-275.

[34] S. Wei, P.W. Tien, Y. Wu, J.K. Calautit, A coupled deep learning-based internal heat gains detection and prediction method for energy-efficient office building operation, Journal of Building Engineering, 47 (2022) 103778.

[35] J. An, D. Yan, T. Hong, K. Sun, A novel stochastic modeling method to simulate cooling loads in residential districts, Applied Energy, 206 (2017) 134-149.

[36] R. Elsland, I. Peksen, M. Wietschel, Are Internal Heat Gains Underestimated in Thermal Performance Evaluation of Buildings?, Energy Procedia, 62 (2014) 32-41.

[37] Y. Ding, Q. Zhang, Z. Wang, M. Liu, Q. He, A simplified model of dynamic interior cooling load evaluation for office buildings, Applied Thermal Engineering,

108   (2016) 1190-1199.

[38]   Roger B. Nelsen, An Introduction to Copulas, second ed., Springer Science+Business Media, Inc, New York, 2006.

[39]   H. Tahir, J.-S. Lee, R.-Y. Kim, Efficiency evaluation of the microgrid for selection of common bus using copula function-based efficiency curves of the converters, Sustainable Energy Technologies and Assessments, 48   (2021) 101621.

[40]   F. Huang, C.G. Ochoa, X. Chen, Assessing environmental water requirement for groundwater-dependent vegetation in arid inland basins by combining the copula joint distribution function and the dual objective optimization: An application to the Turpan Basin, China, Science of The Total Environment, 799   (2021) 149323.

[41]   Y Lu. Practical heating and air conditioning design manual (in Chinese). 2nd ed. Beijing: China building industry;2007.

[42]   J.C.S. Garcia, H. Tanaka, N. Giannetti, Y. Sei, K. Saito, M. Houfuku, R. Takafuji, Multiobjective geometry optimization of microchannel heat exchanger using real-coded genetic algorithm, Applied Thermal Engineering, 202   (2022) 117821.

[43]   K. Deb, A. Pratap, S. Agarwal, T. Meyarivan, A fast and elitist multiobjective genetic algorithm: NSGA-II, IEEE Transactions on Evolutionary Computation, 6 (2) (2002) 182-197.

[44]   H. Chen, P. Hofbauer, J.P. Longtin, Multi-objective optimization of a free-piston Vuilleumier heat pump using a genetic algorithm, Applied Thermal Engineering, 167   (2020) 114767.

[45]   R. Tariq, C.E. Torres-Aguilar, J. Xamán, I. Zavala-Guillén, A. Bassam, L.J. Ricalde, O. Carvente, Digital twin models for optimization and global projection of building-integrated solar chimney, Building and Environment,   (2022) 108807.

[46]   H.-W. Wu, E.-q. Li, Y.-y. Sun, B.-t. Dong, Research on the operation safety evaluation of urban rail stations based on the improved TOPSIS method and entropy weight method, Journal of Rail Transport Planning & Management, 20 (2021) 100262.

[47]   Y. Cheng, J. Niu, N. Gao, Stratified air distribution systems in a large lecture theatre: A numerical method to optimize thermal comfort and maximize energy saving, Energy and Buildings, 55   (2012) 515-525.

[48]   S. Bai, Y. Zhang, L. Li, N. Shan, X. Chen, Effective link prediction in multiplex networks: A TOPSIS method, Expert Systems with Applications, 177   (2021) 114973.

[49]   V.d.A. Guimarães, I.C. Leal Junior, M.A.V. da Silva, Evaluating the sustainability of urban passenger transportation by Monte Carlo simulation, Renewable and Sustainable Energy Reviews, 93   (2018) 732-752.

[50]   American Society of Heating, Refrigerating and Air-Conditioning Engineers,

ASHRAE Handbook Fundamentals 2017. New York, 2017.

[51] J. Chaney, E. Hugh Owens, A.D. Peacock, An evidence based approach to determining residential occupancy and its role in demand response management, Energy and Buildings, 125   (2016) 254-266.

[52] G. Jiefan, X. Peng, P. Zhihong, C. Yongbao, J. Ying, C. Zhe, Extracting typical occupancy data of different buildings from mobile positioning data, Energy and Buildings, 180   (2018) 135-145.

[53] T. Hong, D. Yan, S. D'Oca, C.-f. Chen, Ten questions concerning occupant behavior in buildings: The big picture, Building and Environment, 114   (2017) 518-530.

[54] Ministry of Housing and Urban-Rural Development of the People's Republic of China, GB 55015-2021. General Specification for Building Energy Efficiency and Renewable Energy Utilization, Beijing, 2015.

[55] American Society of Heating, Refrigerating and Air-Conditioning Engineers, ASHRAE Standard 90.1-2019. New York, 2019.

[56] German Institute for Standardization, DIN V 18599-2016. Energy efficency of buildings—Calculation of the energy needs, delivered energy and primary energy for heating, cooling, ventilation, domestic hot water and lighting, Berlin, 2018.

[57] Ministry of Housing and Urban-Rural Development of the People's Republic of China, GB 50034-2013. Standard for lighting design of buildings, Beijing, 2013.

[58] The IESNA Office Lighting Committee, ANSI/IESNA RP-1-04. American National Standard Practice for Office Lighting, New York, 2004.

[59] German Institute for Standardization, DIN 5035-1. Artificial Lighting Terminology and General Requirement, Berlin, 1990.

[60] S.M.A. Hosseini, L. Farahzadi, O. Pons, Assessing the sustainability index of different post-disaster temporary housing unit configuration types, Journal of Building Engineering, 42   (2021) 102806.

Appendix A

Questionnaire of occupant behavior in office buildings

1. Your department is （）

2. Your office hours on weekdays are （）

Your office hours on weekends are （）

3. Your main activities in the office are （）

Standing at work/ Standing or walking slightly/ Walking frequently/ Laboratory experiment

4. The thermal sensation before you choose to open the window for ventilation is （）

Moderate/ Slightly hot/ Hotter/ Very hot

5. Your usage of the office equipment is （）

Mainly use your own equipment/ Mainly use office equipment/ Both

6. What equipment do you use in your office? (Only fill in the equipment you use frequently.)

Desktop/ Laptop/ Mini printer/ Water dispenser/ Large printer/ Thredder/ Air purifier/ refrigerator/ Kettle

7. On weekdays, how long do you turn on your laptop in the office ( )h, use your laptop in the office ( )h, standby your laptop in the office ( )h.

8. On weekdays, how long do you turn on your desktop in the office ( )h, use your desktop in the office ( )h, standby your desktop in the office ( )h.

9. How often do you use small printers, water dispensers, large printers, shredders, air purifiers, refrigerators, and kettles?

Kettle ( )

1-3 times/day   4-6 times/day   7-9 times/day   More than 10 times/day

Shredders ( )

Less than 1 time/day   1-3 times/day   4-6 times/day   7-9 times/day   10-20 times/day   More than 21 times/day

10. Do you have the habit of napping?

Yes, napping in the office, the time period is ( )

Yes, not napping in the office, the time period is ( )

No, in the office at noon, the time period is ( )

No, not in the office at noon, the time period is ( )

11. How long will you leave the room when you choose to turn off the lights?

10min   30min   60min   120min   More than 120min

12. What do you choose to do with your computer under different absence period? (Keep, Standby, Lock, Turn off)

0-0.5 h   0.5-2 h   2-24 h

13. What do you wear in different outdoor temperature? (General outerwear, Summer clothes, Work clothes）

20~23 ℃   23~26 ℃   26~29 ℃   29~32 ℃   32~35 ℃

14. Do you choose to open the lights under different indoor illumination? (Moring, Noon, Afternoon)

0~25 lux   25~50 lux   50~75 lux   75~100 lux

Appendix B

Table B. Design parameters for office building C in building energy simulation

Building type	Office
Floor area (m^2)	3690/10238
Window-to-Wall ratio	28.94%/28.84%
Weather data	Parameters of typical meteorological year in Tianjin
Envelope performance parameters	
Exterior walls (W/m^2*K)	0.35
Ground floor (W/m^2*K)	0.25
Roof (W/m^2*K)	0.25
Window (W/m^2*K)	1.96
HVAC system	
Heating type	Gas furnace inside the packaged air conditioning unit
Cooling type	Packaged air conditioning unit
HVAC sizing	Autosized with design day
Used fuel types	Gas and electricity
Thermostat setpoint	22℃ heating/26℃ cooling
Thermostat setback	15℃ heating/30℃ cooling

Declaration of interests

☐ The authors declare that they have no known competing financial interests or personal relationships that could have appeared to influence the work reported in this paper.

☒ The authors declare the following financial interests/personal relationships which may be considered as potential competing interests:

Yan Ding reports financial support was provided by Natural Science Foundation of Tianjin Science and Technology Correspondent Project. Yan Ding: Conceptualization, Methodology, Writing- Reviewing and Editing. Junchu Li: Formal analysis, Visualization, Writing- Original draft preparation. Shen Wei: Visualization, Writing- Reviewing and Editing. Kuixing Liu: Resources, Data curation. Shuxue Han: Investigation, Modeling. All co-authors have seen and agree with the contents of the manuscript and there is no financial interest to report. We certify that the submission is original work and is not under review at any other publication. I testify to the accuracy of the above on behalf of all the authors.